

# Masked Generative Transformer Is What You Need for Image Editing

Wei Chow<sup>1,2,\*</sup> Linfeng Li<sup>1,\*</sup> Xian Sun<sup>3</sup> Lingdong Kong<sup>1,2</sup> Zefeng Li<sup>1</sup> Qi Xu<sup>1</sup>  
 Hang Song<sup>1</sup> Tian Ye<sup>5</sup> Xian Wang<sup>1</sup> Jinbin Bai<sup>2</sup> Shilin Xu<sup>1</sup> Xiangtai Li<sup>1</sup>  
 Juntong Pan<sup>1</sup> Shaoteng Liu<sup>1</sup> Ran Zhou<sup>1</sup> Tianshu Yang<sup>1</sup> Songhua Liu<sup>4,†</sup>

<sup>1</sup>ByteDance <sup>2</sup>National University of Singapore <sup>3</sup>Duke University <sup>4</sup>Shanghai Jiao Tong University <sup>5</sup>HKUST(GZ)

🌐 **Project Page, Code & Dataset:** <https://weichow23.github.io/EditMGT>

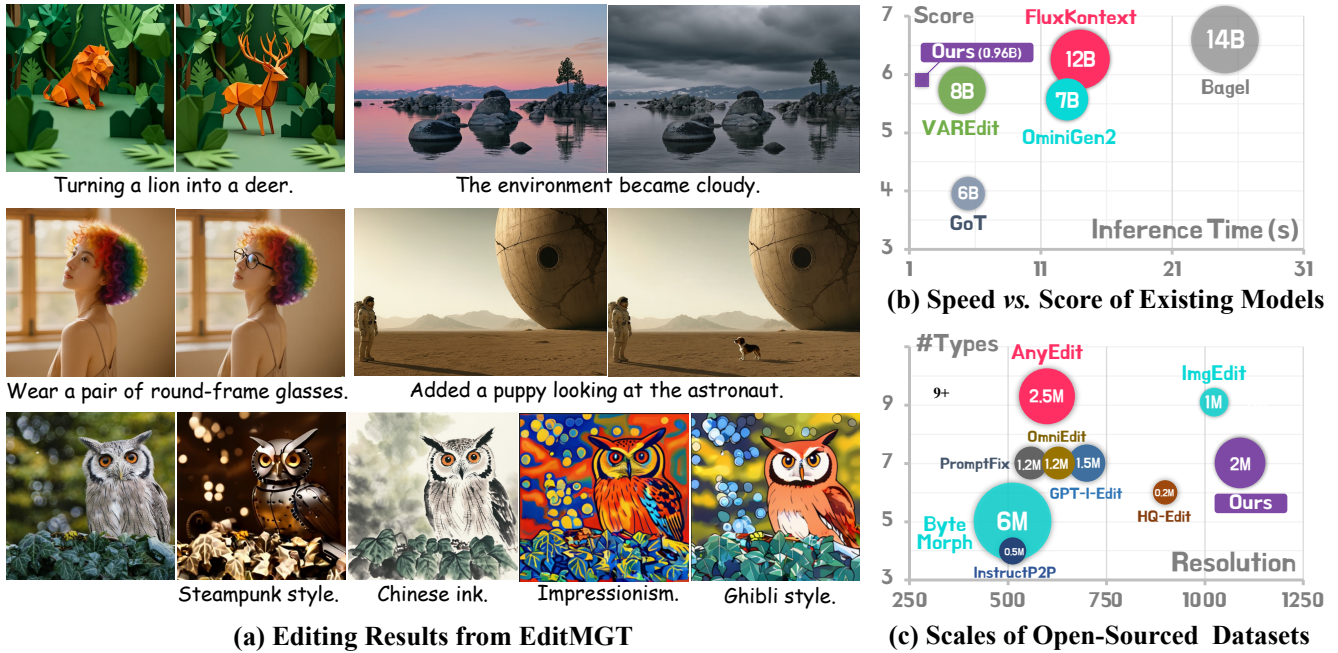


Figure 1. **Overview of EditMGT and CrispEdit-2M.** We introduce the first MGT-based editing model that performs editing in 2s with 960M parameters,  $6\times$  faster than existing models of comparable performance while surpassing 8B models. We also contribute CrispEdit-2M, providing 2M high-resolution ( $\geq 1024$ ) editing samples across 7 categories.

## Abstract

Diffusion models dominate image editing, yet their global denoising mechanism entangles edited regions with surrounding context, causing modifications to propagate into areas that should remain intact. We propose a fundamentally different approach by leveraging Masked Generative Transformers (MGTs), whose localized token-prediction paradigm naturally confines changes to intended regions. We present *EditMGT*, an MGT-based editing framework that is the first of its kind. Our approach employs multi-layer attention consolidation to aggregate cross-attention maps into precise edit localization signals, and region-hold sampling to explicitly prevent token flipping in non-target areas. To support training, we construct *CrispEdit-2M*, a 2M-sample high-resolution ( $\geq 1024$ ) editing dataset spanning seven categories. With only 960M param-

eters, *EditMGT* achieves state-of-the-art image similarity on multiple benchmarks while delivering  $6\times$  faster editing, demonstrating that MGTs offer a compelling alternative to diffusion-based editing.

## 1. Introduction

Instruct a diffusion model to “put a birthday hat on the dog”, and you may find the dog’s fur subtly recolored, the background shifted, or the lighting altered in ways you never requested. This *edit leakage* stems from the global denoising dynamics of diffusion models (DMs) [8]: every step refines the entire image simultaneously, making it inherently difficult to confine modifications to a specific region. Prior solutions based on large-scale training [21], predefined masks [22], or inversion techniques [12] mitigate but do not fully resolve this entanglement.

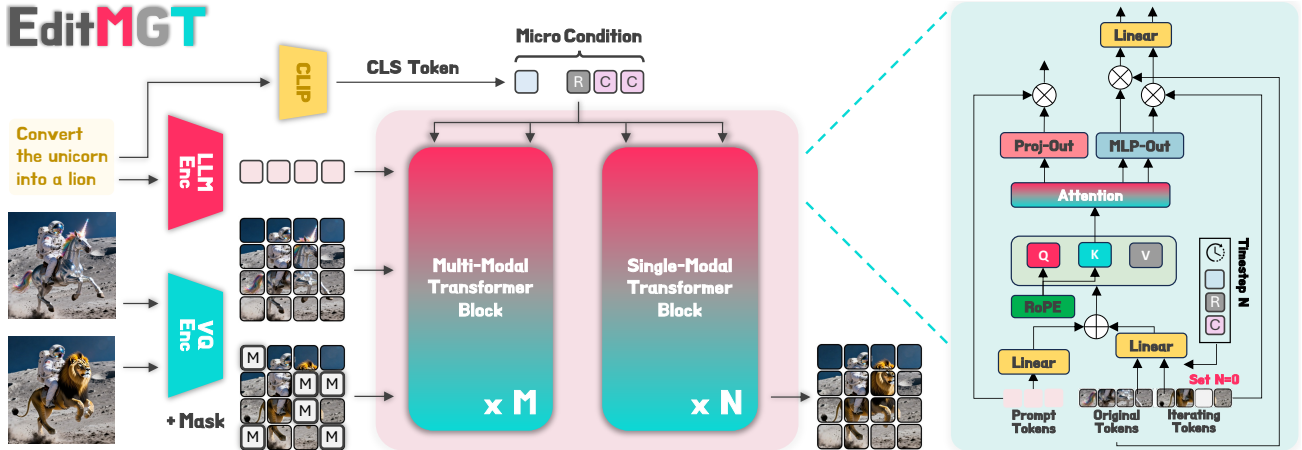


Figure 2. **EditMGT framework.** The original image conditions generation via attention injection. Right panel: token interactions inside the multi-modal and single-modal transformer blocks.

We observe that a different class of generative models sidesteps this problem entirely. Masked Generative Transformers (MGTs) [3] synthesize images by iteratively predicting masked tokens in parallel rather than performing holistic refinement. This localized decoding paradigm naturally supports selective token replacement: tokens corresponding to non-target regions can simply be held fixed, providing an architectural guarantee against edit leakage that DMs lack. The question here is whether this token-level control can be harnessed for high-quality, instruction-driven image editing.

We answer affirmatively with **EditMGT** [5], an MGT-based editing framework that is, to our knowledge, the first of its kind. We aim to address two essential capabilities for effective editing. First, for *adaptive localization*, we find that MGT cross-attention maps encode informative semantic correspondences between text instructions and visual regions, but lack sufficient prominence for direct use. We devise *multi-layer attention consolidation* that aggregates and refines these maps across network layers, producing sharp, accurate localization of edit-relevant areas (Fig. 3). Second, for *region preservation*, we propose *region-hold sampling*, a strategy that restricts token updates within low-attention areas during iterative decoding, explicitly preventing modifications from propagating into non-target regions. To train EditMGT, we assemble CrispEdit-2M, a high-resolution ( $\geq 1024$ ) editing dataset with 2M rigorously filtered samples across seven distinct categories. We adapt a pretrained text-to-image MGT (Meisssonc [1]) into an editing model via attention injection, requiring no additional parameters.

## 2. Methodology

**Preliminary: Masked Generative Transformers.** MGTs synthesize images by starting from a fully masked token grid and progressively revealing tokens via parallel predic-

tion and confidence-based resampling [3]. Let  $C_I \in \mathbb{R}^{N \times d}$  and  $C_T \in \mathbb{R}^{M \times d}$  denote image and text tokens. Building upon Meisssonc [1], each transformer block applies RoPE [15] for spatial encoding, then computes multi-modal attention over  $C = [C_I; C_T]$ :  $\mathbf{W} = \text{softmax}(QK^T / \sqrt{d})$ . This token-level control makes MGTs naturally suited for editing: tokens in non-target regions can remain fixed throughout decoding.

**Image-Conditioned Editing via Attention Injection.** To condition the generation on the original image, we introduce image condition tokens  $C_V \in \mathbb{R}^{N \times d}$  with the same shape as  $C_I$  (Fig. 2). Critically,  $C_V$  shares all parameters with  $C_I$  and uses identical RoPE positions, *i.e.*,  $(i, j)_{C_V} = (i, j)_{C_I}$ , ensuring precise spatial alignment between the source and edited images. The key distinction is that the timestep assigned to  $C_V$  is held constant at zero, preventing temporal drift and maintaining a stable reference signal.

The model  $\theta$  is trained by minimizing the cross-entropy loss over masked token reconstruction, jointly conditioned on visible tokens and the image reference:

$$L = \mathbb{E}_{(x,t) \sim \mathcal{D}, \mathbf{m} \sim \mathcal{M}} \left[ - \sum_{i \in \mathbf{m}} \log p_{\theta}(v_i | v_{\neg i}, C_T; C_V) \right], \quad (1)$$

where  $\mathbf{m}$  is a binary mask selecting tokens to predict,  $v_{\neg i}$  denotes visible tokens, and the masking rate follows a cosine schedule sampled from a truncated arccos distribution. To control  $C_V$ 's influence at inference, we introduce a bias matrix  $\mathcal{E}$  into the attention weights as  $\mathbf{W}_{\text{new}} = \mathbf{W} + \mathcal{E}$ , where  $\mathcal{E}$  scales attention between  $C_I$  and  $C_V$  by  $\log(\gamma)$  while leaving intra-modality patterns unchanged. Setting  $\gamma = 0$  removes conditioning;  $\gamma > 1$  strengthens it. This mechanism transforms the pretrained text-to-image MGT into an editor via attention injection alone, without introducing any additional parameters.

**Multi-Layer Attention Consolidation.** We find that the cross-attention weights between instruction tokens  $C_T$  and

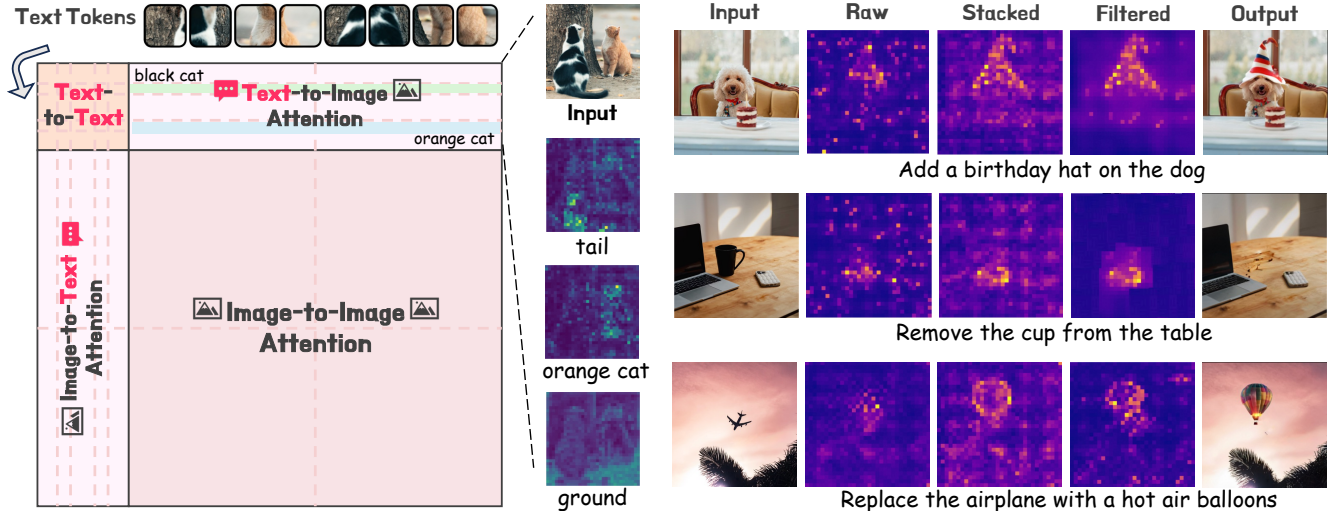


Figure 3. **Attention mechanism in EditMGT.** Cross-attention maps encode semantic correspondences between instructions and visual regions. Multi-layer consolidation sharpens these maps for region-hold sampling.

Table 1. **Comparative results** for instructive image editing on the test sets of EMU Edit [14] and MagicBrush [22]. We list the task-specific models in the first block and some concurrent universal models in the second block.

Model	Venue	Size	EMU Edit Test Set				MagicBrush Test Set			
			CLIP <sub>im</sub> ↑	CLIP <sub>out</sub> ↑	L1↓	DINO↑	CLIP <sub>im</sub> ↑	CLIP <sub>out</sub> ↑	L1↓	DINO↑
• InstructPix2Pix [2]	CVPR'23	1B	0.834	0.219	0.121	0.762	0.837	0.245	0.093	0.767
• MagicBrush [22]	NeurIPS'23	1B	0.838	0.222	0.100	0.776	0.883	0.261	0.058	0.871
• PnP [17]	CVPR'23	1B	0.521	0.089	0.304	0.153	0.568	0.101	0.289	0.220
• Null-Text Inv. [12]	CVPR'23	1B	0.761	0.236	0.075	0.678	0.752	0.263	0.077	0.664
• UltraEdit [23]	NeurIPS'24	2B	0.793	0.283	0.071	<b>0.844</b>	0.868	-	0.088	0.792
• EMU Edit [14]	CVPR'24	-	0.859	0.231	0.094	0.819	0.897	0.261	<u>0.052</u>	<u>0.879</u>
• AnyEdit [21]	CVPR'25	1B	0.872	0.285	<u>0.070</u>	0.821	0.898	0.275	<b>0.051</b>	0.881
• OmniGen [20]	arXiv'24	4B	0.836	0.233	-	0.804	-	-	-	-
• PixWizard [9]	ICLR'25	2B	0.845	0.248	<b>0.069</b>	0.798	0.884	0.265	0.063	0.876
• UniReal [4]	CVPR'25	5B	0.851	0.285	0.099	0.790	<u>0.903</u>	<b>0.308</b>	0.081	0.837
• GoT [7]	NeurIPS'25	6B	0.864	0.276	-	-	-	-	-	-
• OminiGen2 [18]	arXiv'25	7B	<u>0.876</u>	<b>0.309</b>	-	0.822	-	-	-	-
• EditAR [13]	ICLR'25	3B	-	-	-	-	0.867	-	0.103	0.804
• NEP [19]	arXiv'25	3B	0.871	0.307	0.078	<b>0.844</b>	-	-	-	-
• VAREdit [11]	arXiv'25	8B	<u>0.876</u>	0.280	0.094	0.825	0.901	0.287	0.083	0.844
• <b>EDITMGT</b>	<b>Ours</b>	1B	<b>0.878</b>	<u>0.308</u>	0.093	<u>0.832</u>	0.911	<u>0.301</u>	0.058	<b>0.881</b>

image tokens  $C_I$  naturally encode the spatial location of intended edits (Fig. 3). Notably, even within the initial iterations, the model can delineate the contours of objects to be added or modified, establishing precise text-to-image correspondence. However, individual layer activations lack sufficient prominence and exhibit unclear boundaries with internal discontinuities, making them unreliable for direct use as localization masks.

To remedy this, we aggregate attention from the most coherent single-modality processing layers (blocks 28–36), which we empirically identify as producing the most semantically aligned activations. The aggregated map is further refined via adaptive filtering [6] to suppress spatial discontinuities and sharpen object boundaries. The resulting

consolidated map provides a reliable per-token localization signal that distinguishes edit-relevant regions from those that should remain intact.

**Region-Hold Sampling.** Given the consolidated attention map, we compute a localization score for each image token:

$$s_L = \frac{1}{|\mathcal{L}||\mathcal{M}|} \sum_{\ell \in \mathcal{L}, m \in \mathcal{M}} \mathcal{W}_i^\ell[m, :] \in \mathbb{R}^N, \quad (2)$$

where  $\mathcal{W}_i^\ell \in \mathbb{R}^{M \times N}$  is the normalized instruction-to-image attention at layer  $\ell$ ,  $\mathcal{L}$  is the set of selected layers, and  $\mathcal{M}$  indexes the relevant instruction tokens (which can be restricted to specific keywords for finer control). During iterative decoding, the MGT reveals high-confidence tokens while re-masking uncertain ones. With region-hold sam-

pling, tokens satisfying  $s_L < \lambda$  are additionally restored to their original values from  $C_V$  after each step, where  $\lambda$  is a user-controllable threshold that trades off edit extent against preservation.

**Training Pipeline.** We assemble CrispEdit-2M comprising 2M high-resolution ( $\geq 1024$ ) editing samples across seven categories with rigorous quality filtering. Training proceeds in three stages: (1) base model adaptation with Gemma2-2B [16] as text encoder (5K steps), (2) full fine-tuning on 4M editing samples (50K steps), and (3) high-quality refinement for human preference alignment (1K steps). Additional details are available in the main paper [5].

### 3. Experiments

We evaluate **EditMGT** on standard benchmarks: Emu Edit [14], MagicBrush [22], AnyBench [21], and GEdit-EN-full [10]. Details are available in the main paper [5].

**Quantitative Results.** As reported in Table 1, EditMGT achieves state-of-the-art  $CLIP_{in}$  scores on both Emu Edit (0.878) and MagicBrush (0.911), with a 1.1% improvement over the next best method on MagicBrush. DINO scores are state-of-the-art on MagicBrush and second-best on Emu Edit, while instruction adherence ( $CLIP_{out}$ ) remains consistently competitive. On the GPT-based GEdit-EN-full benchmark [10], EditMGT achieves competitive performance with FluxKontext.dev (12B) and surpasses VAREdit-8B, GoT-6B, and OminiGen2-7B, with notable margins of +9.8% on color alteration and +17.6% on style transfer. These results confirm that the MGT’s localized decoding paradigm effectively prevents modifications from propagating into non-target regions.

**Qualitative Results & Efficiency.** Fig. 4 compares EditMGT against UltraEdit (SD3), GoT (6B), OminiGen2 (7B), and VAREdit (8B). Key advantages include superior instruction comprehension (correctly reducing warm tones rather than increasing yellow) and faithful structural preservation (maintaining subject pose during style transfer). At  $1024 \times 1024$  resolution, EditMGT completes an edit in  $\sim 2$  seconds with 13.8 GB memory,  $6 \times$  faster than models of comparable quality.

### 4. Conclusion

We presented **EditMGT**, the first MGT-based framework that resolves the edit leakage problem inherent in diffusion models by leveraging localized token prediction. Multi-layer attention consolidation provides precise, mask-free edit localization, while region-hold sampling preserves non-target content during decoding. With 960M parameters and 2-second inference, EditMGT achieves state-of-the-art similarity across multiple benchmarks and competitive quality with models up to  $12 \times$  larger, establishing MGTs as an efficient paradigm for interactive image editing.

### References

- [1] Jinbin Bai et al. Meissonic: Revitalizing masked generative transformers for efficient high-resolution text-to-image synthesis. *arXiv preprint arXiv:2410.08261*, 2024.
- [2] Tim Brooks et al. InstructPix2Pix: Learning to follow image editing instructions. In *CVPR*, pages 18392–18402, 2023.
- [3] Huiwen Chang et al. MaskGiT: Masked generative image transformer. In *CVPR*, pages 11315–11325, 2022.
- [4] Xi Chen et al. UniReal: Universal image generation and editing via learning real-world dynamics. *arXiv preprint arXiv:2412.07774*, 2024.
- [5] Wei Chow et al. EditMGT: Unleashing potentials of masked generative transformers in image editing. In *CVPR*, 2026.
- [6] Paulo SR Diniz et al. *Adaptive filtering*. Springer, 1997.
- [7] Rongyao Fang et al. GoT: Unleashing reasoning capability of multimodal large language model for visual generation and editing. *arXiv preprint arXiv:2503.10639*, 2025.
- [8] Amir Hertz et al. Prompt-to-prompt image editing with cross attention control. *arXiv preprint arXiv:2208.01626*, 2022.
- [9] Weifeng Lin et al. PixWizard: Versatile image-to-image visual assistant with open-language instructions. *arXiv preprint arXiv:2409.15278*, 2024.
- [10] Shiyu Liu et al. Step1x-Edit: A practical framework for general image editing. *arXiv preprint arXiv:2504.17761*, 2025.
- [11] Qingyang Mao et al. Visual autoregressive modeling for instruction-guided image editing. *arXiv preprint arXiv:2508.15772*, 2025.
- [12] Ron Mokady et al. Null-text inversion for editing real images using guided diffusion models. In *CVPR*, 2023.
- [13] Jiteng Mu et al. EditAR: Unified conditional generation with autoregressive models. In *CVPR*, pages 7899–7909, 2025.
- [14] Shelly Sheynin et al. Emu edit: Precise image editing via recognition and generation tasks. In *CVPR*, pages 8871–8879, 2024.
- [15] Jianlin Su et al. Roformer: Enhanced transformer with rotary position embedding. *Neurocomputing*, 568:127063, 2024.
- [16] Gemma Team et al. Gemma 2: Improving open language models at a practical size. *arXiv preprint arXiv:2408.00118*, 2024.
- [17] Narek Tumanyan et al. Plug-and-play diffusion features for text-driven image-to-image translation. In *CVPR*, pages 1921–1930, 2023.
- [18] Chenyuan Wu et al. OmniGen2: Exploration to advanced multimodal generation. *arXiv preprint arXiv:2506.18871*, 2025.
- [19] Huimin Wu et al. NEP: Autoregressive image editing via next editing token prediction. *arXiv preprint arXiv:2508.06044*, 2025.
- [20] Shitao Xiao et al. OmniGen: Unified image generation. In *CVPR*, pages 13294–13304, 2025.
- [21] Qifan Yu et al. AnyEdit: Mastering unified high-quality image editing for any idea. In *CVPR*, 2025.
- [22] Kai Zhang et al. MagicBrush: A manually annotated dataset for instruction-guided image editing. *NeurIPS*, 36, 2024.
- [23] Haozhe Zhao et al. UltraEdit: Instruction-based fine-grained image editing at scale. *arXiv preprint arXiv:2407.05282*, 2024.

